



**HAL**  
open science

## Ultrasound and microbubble-assisted gene delivery: insights for intracellular mechanism

Anthony Delalande, Spiros Kotopoulos, Patrick Midoux, Michiel Postema,  
Chantal Pichon

► **To cite this version:**

Anthony Delalande, Spiros Kotopoulos, Patrick Midoux, Michiel Postema, Chantal Pichon. Ultrasound and microbubble-assisted gene delivery: insights for intracellular mechanism. Micro-acoustics in marine and medical research: 1st workshop, Dec 2011, Bergen, Norway. pp.119-130, 10.5281/zenodo.4779438 . hal-03197797v2

**HAL Id: hal-03197797**

**<https://hal.science/hal-03197797v2>**

Submitted on 21 May 2021

**HAL** is a multi-disciplinary open access archive for the deposit and dissemination of scientific research documents, whether they are published or not. The documents may come from teaching and research institutions in France or abroad, or from public or private research centers.

L'archive ouverte pluridisciplinaire **HAL**, est destinée au dépôt et à la diffusion de documents scientifiques de niveau recherche, publiés ou non, émanant des établissements d'enseignement et de recherche français ou étrangers, des laboratoires publics ou privés.

# 9

## Ultrasound and microbubble-assisted gene delivery: insights for intracellular mechanism

Anthony Delalande<sup>1,2</sup>, Spiros Kotopoulos<sup>3,2</sup>, Patrick  
Midoux<sup>4</sup>, Michiel Postema<sup>2</sup>, Chantal Pichon<sup>4</sup>

<sup>1</sup>Department of Haematology, Haukeland hospital, Bergen, Norway

<sup>2</sup>Department of Physics and Technology, University of Bergen, Bergen, Norway

<sup>3</sup>Department of Gastroenterology, Haukeland hospital, Bergen, Norway

<sup>4</sup>Centre de Biophysique Moléculaire, CNRS, Orléans, France

---

### Abstract

Microbubbles are capable to oscillate under specific ultrasound settings that can lead to a permeabilisation of surrounding cells and this phenomenon is called sonoporation. The sonoporation technique has been used to deliver drugs *in vitro* and *in vivo* for gene or chemotherapeutic drug delivery applications. However, the biological and physical mechanisms of sonoporation are still not fully understood. We have used a luciferase reporter plasmid to identify the optimal parameters for an efficient gene delivery in human cancer HeLa cells. The optimal parameters found at 1 MHz were 150 kPa, 40% duty cycle, 60 sec sonication time using 0.3% of microbubbles. The interactions between microbubbles and cells were investigated by high-speed imaging during sonoporation. Specifically at 150 kPa, microbubbles entry into cells has been observed during sonoporation. These results strongly suggest that the microbubble entry could be closely correlated to the plasmid DNA entry into the cell. The intracellular kinetic of the plasmid delivery was followed by confocal microscopy using fluorescent molecules and specific cell markers for late endosomes and nuclear envelope. Most of plasmids

were located in late endosomes 3 hours after sonoporation and some could reach the nucleus 3 hours later. The gene transfer efficiency was almost totally inhibited when depleting the cell ATP and in presence of chlorpromazine suggesting that plasmid uptake after sonoporation was an active mechanism mostly involving the clathrin-mediated pathway.

---

## Introduction

Gene delivery by non-viral methods is still a major challenge nowadays. It offers a great promise for gene therapy because of its safety compared to their viral counterparts. However, a major limiting factor for efficient non-viral gene therapy remains the lack of a suitable and efficient vector for gene delivery. Fifteen years ago, a new drug delivery method based on ultrasound stimulation coupled to gaseous microbubbles has been proposed. Upon ultrasound exposure, microbubbles can be expanded, moved and even destroyed [1] and can modify the cell membrane permeability by a process known as sonoporation [2-4]. These properties offer the opportunity of site-specific local delivery of drug or gene. Although the mechanism of membrane permeabilization has not been clearly elucidated, the main hypothesis assumes the formation of transient pores in the plasma membrane as a consequence of interaction of oscillating microbubbles with the cell membrane [3-5]. Transient pores formed at the plasma membrane are supposed to be responsible for the intracellular delivery of molecules but also the outward transport of intracellular molecules [6]. Recently, two studies have shown that endocytosis process could also be involved in the sonoporation mechanism for large molecules [7, 8]. In the field of gene transfer, several studies have reported an improvement of gene delivery efficiency by sonoporation [9]. Numerous studies on sonoporation *in vitro* and *in vivo* and its exploitation for gene transfer have been reported [5, 10, 11]. However, the mechanisms of gene transfer from microbubble stimulation to protein expression are not well understood. Previous studies have shown that pore membrane formation could occur during sonoporation [5]. This study is focused on optimal ultrasound parameters determination for efficient gene transfer *in vitro*, microbubbles and cell interactions observation during sonoporation and plasmid DNA and microbubbles intracellular trafficking following sonoporation.

## Materials and Methods

### **Cell culture**

HeLa cells are adherent human epithelial cells from a fatal cervical carcinoma (ATCC, Rockville, MD). They were grown in MEM with Earl's salts medium (PAA Laboratories GmbH, Pasing, Austria) supplemented with 10% v/v of FCS and 1% of non essential aminoacids (PAA), penicillin (100 U/ml) and streptomycin (100 µg/ml) at 37°C in a humidified atmosphere containing 5% CO<sub>2</sub>. HeLa cells stably expressing the fusion protein Rab7-GFP and Nup153-GFP were developed to localise the fluorescent-labelled plasmid DNA into specific cellular structures.

### **Plasmid preparation and labelling**

A 7.5 kb homemade reporter plasmid that encoded the firefly luciferase gene (pLuc) under the control of the strong cytomegalovirus promoter was used. Five consecutive NF $\kappa$ B motifs that recognized the NF $\kappa$ B transcription factor were inserted upstream of the promoter [12]. All plasmids were propagated from *Escherichia coli* DH5 $\alpha$  cultures. Supercoiled plasmid was isolated from bacteria by the standard alkaline lysis method, and purification was carried out with the Qiagen Mega Kit (Qiagen, Courtabœuf, France) according to the manufacturer's instructions. Each plasmid DNA was labelled with the Label IT nucleic acid labelling kit (Mirus, Madison, WI, USA) at 1:2 reagent/pDNA weight ratio according to manufacturer's instructions. Plasmids were labelled with cyanine 3 ( $\lambda_{ex}$ = 543 nm,  $\lambda_{em}$ = 570 nm) and DNA was purified by ethanol precipitation. The labelling densities determined by absorbance according to the manufacturer's protocol were 1 cyanine 3 per 80 bp. We have verified that this type of plasmid labelling did not affect the gene expression.

### ***Ultrasound exposure system for gene transfer***

US were generated from a 0.5-inch diameter, IBMF-014 transducer with a centre frequency of 1 MHz (Sofranel, Sartrouville, France). The transducer was placed in a custom made polystyrene tank filled with degassed pure water. A signal consisting of 1.0 MHz centre frequency, 40% duty cycle and a pulse repetition frequency of 10 kHz was generated by a 33220A arbitrary function generator (Agilent technologies, Les Ulis, France) and amplified by a RF power amplifier (ADECE, Artannes sur Indre, France) was used as the input for the transducer. Peak negative pressure of 150 kPa was used corresponding to an MI of 0.15. Ultrasound stimulation time was set to 60 seconds. The transducer was calibrated in a Perspex container using an HGL-200 PVDF bullet type hydrophone (Onda, Sunnyvale, CA) placed at 3 cm, the natural focal distance of the transducer. The transducer was positioned in front of the sonoporation cuvette (Sarstedt AG & Co, Nümbrecht, Germany). The attenuation of the cuvette walls was measured separately and found to be negligible (less than 10%). 10<sup>5</sup> cells were grown on a resized Opticell<sup>®</sup> membrane (10×15 mm) (Nunc GmbH & Co. KG, Langenselbold, Germany). The Opticell<sup>®</sup> membranes were transferred into polystyrene cuvettes (Sarstedt, Nümbrecht, Germany) containing 1.5 ml of OptiMEM medium (Invitrogen, Carlsbad, CA, USA) supplemented with 1% FCS. During sonoporation the cell medium was placed under gentle agitation using a magnetic stirrer. After sonoporation the membrane was placed in a 12-well cell culture plate.

### ***Ultrasound exposure system for high-speed imaging***

For fast camera imaging experiments, the transducer was placed in a custom-made aluminum sonication chamber with internal dimensions of 130×170×35 (mm)<sup>3</sup> was locked into to the xy-stage of a 200M inverted microscope (Carl Zeiss AG, Oberkochen, Germany) coupled with a LSM Axiovert 510 confocal scanning device (Carl Zeiss), using an EC Plan-Neofluar 40×/1.30. Oil DIC M27 objective (Carl Zeiss AG), with automated z-stack functionality. The colour charge coupled device (CCD) of a Photron FastCam MC-2.1 high-speed camera (VKT Video Kommunikation GmbH, Pfullingen, Germany) was connected to the microscope. The sensor was rotated to make sure that in all recorded movies, the ultrasound is directed from the left to the right of the frame.

The peak-negative acoustic pressures were measured in the insonation tank at the objective's field of view and corresponded to MI of 0.1, 0.15 or 0.2. The day before the experiment  $1.6 \times 10^6$  cells were seeded in an Opticell® chamber. Ultrasound contrast agents were injected into the cell culture chamber before each experiment.

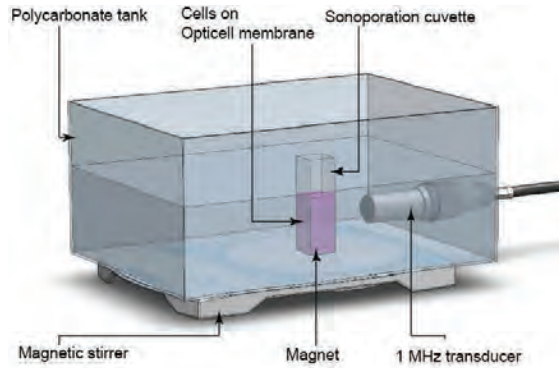


Figure 1 - *In vitro* sonoporation set-up used for gene transfer experiments.

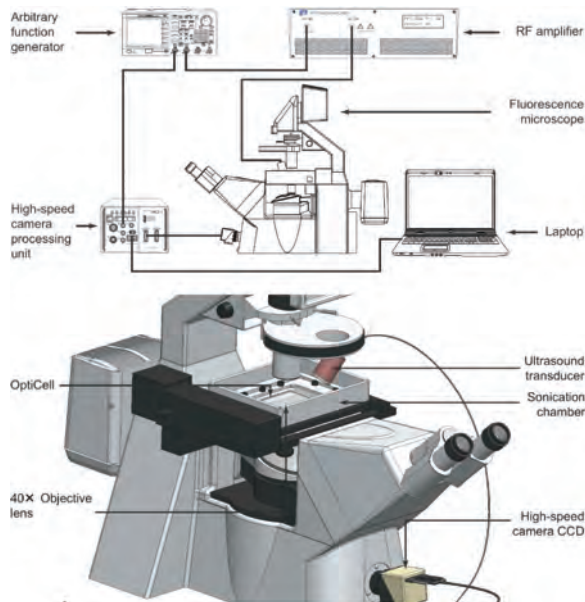


Figure 2 - *In vitro* set-up used for high-speed imaging experiments.

### **Ultrasound contrast agent**

In this study, Micromarker<sup>®</sup> (VisualSonics, La Frette S/Seine, France) microbubbles were used. Micromarker<sup>®</sup> contrast agents contain a perfluorobutane (C<sub>4</sub>F<sub>10</sub>) gas encapsulated by a phospholipid shell and have a median diameter of 2.3 to 2.9 µm. Microbubbles were prepared according to manufacturer's protocol, Micromarker<sup>®</sup> suspension contained approximately 2×10<sup>9</sup> MB/ml.

### **Luciferase activity assay**

The efficiency of sonoporation to deliver gene was determined by measuring the luciferase activity 24 h after sonoporation of HeLa cells in the presence of a plasmid encoding the luciferase reporter gene. Cells were harvested, lysed and the luciferase activity was measured using a luminometer (Lumat LB9507, Berthold, Wildbach, Germany) after adding 100 µl of luciferase substrate (1 mM luciferin containing ATP) to 60 µl of cell lysate. The values were expressed as RLU (Relative Luciferase Unit), this level was reported to the protein concentration in RLU/mg proteins. The protein concentration was measured by the bicinchoninic acid assay.

### **Cell viability assay**

The cell viability was determined 24h after sonoporation using the MTT colorimetric assay. Cells were incubated during 4 h at 37°C, 5% CO<sub>2</sub> in presence of 3-(4,5-dimethylthiazol-2-yl)-2,5-diphenyltetrazolium bromide (Sigma-Aldrich, St. Louis, USA) at 500 µg/ml. Cells were washed and incubated in a lysis and resuspension buffer consisting of acidified isopropanol containing 3% of SDS (Sigma-Aldrich). Quantification was made measuring the optic density at 560 nm.

### **Inhibition of endocytosis during sonoporation**

To evaluate if the gene uptake by sonoporation was an active mechanism, cells were ATP depleted by incubation in presence of ATP depletion buffer (50 mM 2-deoxy-ATP, 50 mM sodium azide, 1.8 mM CaCl<sub>2</sub> in PBS pH 7.4) 30 minutes before the sonoporation. To study the involvement of the endocytosis pathways on the gene delivery mediated by sonoporation, cells were pre-treated for 30 minutes with either chlorpromazin (2.5 to 20 µg/ml; Sigma-Aldrich) an inhibitor of clathrin-mediated endocytosis pathway or filipin III (1 to 4 µg/ml; Sigma-Aldrich) or an inhibitor of caveolin-mediated endocytosis pathway. Then, sonoporation was performed in presence of indicated inhibitor and the cell medium was replaced two hours after sonoporation to maintain the inhibition effect.

### **Microbubble fluorescent labelling**

In order to detect the microbubbles location after sonoporation, the envelope of Micromarker<sup>®</sup> microbubbles was stained with the fluorescent lipophilic probe DiD ( $\lambda_{ex}$ = 633 nm,  $\lambda_{em}$ = 643-670 nm) (Vybrant™, Molecular Probes<sup>®</sup>, Invitrogen, San Diego, CA, USA). A ratio of 1 µl of DiD to 40 µl MicroMarker<sup>®</sup> was used. The solution was homogenised by pipetting and it was used after 5 min incubation at room temperature.

## Results and discussion

### *Optimal acoustic parameters determination for efficient gene transfer.*

The optimal acoustic parameters that give the maximal gene transfer have been first determined on adherent HeLa cells using the set-up described previously. Four parameters were tested: the sound pressure (kPa), time (sec), the duty cycle (%) and the concentration of microbubbles (%). We tested different values of acoustic pressure in having fixed the other parameters tested (60 sec, 40% DC, 0.3% microbubbles). Figure 3A shows the effect of this the acoustic pressure on the gene transfer efficiency from 100 to 200 kPa. Indeed, increasing the acoustic pressure from 100 to 160 kPa caused a linear increase in the efficiency of gene transfer (from  $3.2 \times 10^4$  to  $2 \times 10^6$  RLU/mg prot, increase of about 100 times). The maximum efficiency was obtained at 160 kPa. Beyond 160 kPa, the efficiency of gene transfer was low and at 200 kPa, it reached a value of  $1.9 \times 10^5$  RLU/mg prot which consists of a reduction by about 10 times compared to the highest value. These values were in the same range as that obtained in the study of Duvshani *et al.* performed on mouse prostate adenocarcinoma cells although these experiments have been conducted with Optison™ [13]. In a similar study performed on HeLa cells using SonoVue®, these authors have found that a maximum efficiency of gene transfer was obtained for an ultrasonic stimulation of 240 kPa for 7 minutes with a duty cycle of 60%. However, a high toxicity was measured (30% cell viability) [14]. In our study, the cell viability reached a value of 90% in the optimal condition. The ultrasound exposure time tested was ranged from 10 to 300 seconds. Figure 3B shows that gene transfer efficiency was positively correlated with ultrasound insonation time between 10 and 60 seconds corresponding to an increase from  $2.1 \times 10^4$  to  $5.4 \times 10^5$  RLU/mg prot. A plateau was observed between 60 and 300 seconds. However, it should be noted that a high variability was observed for long stimulation time. This can be explained by an increase in the toxicity induced by sonoporation with time of stimulation. Indeed, we observed a cell toxicity ranging from 30 to 60% for the respective ultrasound stimulation time of 10 and 300 seconds.

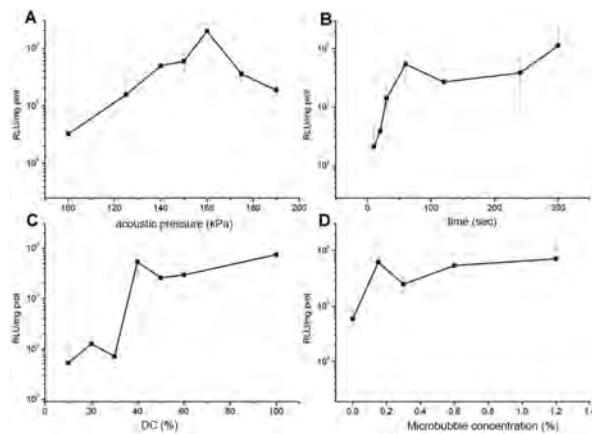


**Figure 3** - Optimal sonoporation parameters determination. (A) Influence of the acoustic pressure (parameters: 0.3% MB, 60 sec, 40% DC, 2.5  $\mu$ g pDNA). (B) Influence of the time of insonation (parameters: 150 kPa, 0.3% MB, 40% DC, 2.5  $\mu$ g pDNA). (C) Influence of the duty cycle (DC) (parameters: 150 kPa, 60 sec, 0.3% MB, 2.5  $\mu$ g pDNA). (D) Influence of the concentration in microbubbles (parameters: 150 kPa, 60 sec, 40% DC, 2.5  $\mu$ g pDNA). Values shown represent means of 3 experiments done in duplicates.

Regarding the duty cycle (Figure 3C), a threshold value of 40% duty cycle was required for an efficient gene transfer. Between 10 and 30% duty cycle, a very low expression level of luciferase was obtained (around  $10^4$  RLU/mg prot). At 40% duty cycle, an increase of 75 times of gene transfer efficiency was obtained. Then a plateau was reached between 40 and 60% duty cycle. However, it should be noted that the experiments conducted at 60% duty cycle led to a high toxicity (60%). This was consistent with our previous results on HeLa cells in suspension in the presence of microbubbles BR14 [15]. In this study, a plateau was reached at 40% duty cycle.

The importance of the amount of microbubbles was also evaluated. Figure 3D showed that the presence of a certain concentration of microbubbles (0.15%) to get a gene delivery. Above this concentration, the transfection efficiency was very dependent on the quantity of microbubbles used. This observation was similar to that we previously obtained on HeLa cells in suspension in the presence of microbubbles BR14 [15] and the study of Rahim *et al.* performed on CHO cells adherent in the presence of SonoVue® [16].

Taken together, the above results reflect the importance of the parameters used in ultrasound effectiveness for gene transfer mediated by sonoporation. Depending on the settings used, the microbubble-cell interactions could be changed. Therefore, we established a sonoporation device coupled to a high-speed camera to observe these interactions in real time.

### ***Microbubble behaviour during sonoporation***

The behaviour of microbubbles during sonoporation was studied by high-speed imaging methods. We performed real-time visualisation of sonoporation event by high-speed imaging to investigate how microbubbles behave towards cells as a function of the acoustic pressure. Possible interactions between microbubbles and cells were investigated using the optimal acoustic parameters (1 MHz, 40% DC, 100  $\mu$ s period, 100 to 200 kPa, 0.3% microbubbles concentration). Figure 4 shows different types of microbubble-cell interactions as a function of sound pressure. Three acoustic pressures were tested (100, 150 and 200 kPa). At 100 kPa, the main observed phenomenon was as a cellular massage. The arrow shows an activated microbubbles by ultrasound remaining in contact with the cell membrane during the whole stimulation (Figure 4A). At this acoustic pressure, a low gene transfer was obtained as seen on Figure 3A. At 150 kPa, an additional phenomenon consisting of the microbubble entry into cells was seen (figure 4B). In the event presented in this sequence, the microbubble enters the cell after 600ms ultrasonic stimulation. Note that at this acoustic pressure range, the optimal efficiency of gene transfer was obtained (Figure 3A). For a sound pressure of 200 kPa, two phenomena were identified: either the microbubbles were driven from the field of view due to excessive radiation force or a violent interaction of microbubbles with the cell was observed. The latter induced a detachment of some cells from their support. It is important to note that at 200 kPa the gene transfer efficiency is ten times lower than at 150 kPa. The results obtained from our real time sonoporation indicate that three events types could be recorded: microbubbles stuck on cell membrane during the insonation corresponding to the cellular massage, microbubbles entering into

cells (translation), microbubbles having a violent interaction with cells. It is tempting to correlate the entry of microbubbles phenomenon and efficiency of gene transfer meaning that the entry of the microbubble could promote the delivery of the plasmid into the cell. Our set up analysis was checked to rule out that the motion of microbubbles takes place in a plane different from that of the cell. This was also validated by fluorescence confocal microscopy analysis. When DiD-labelled microbubbles were used, our observations indicated that microbubbles were inside the cell just below the plasma membrane.

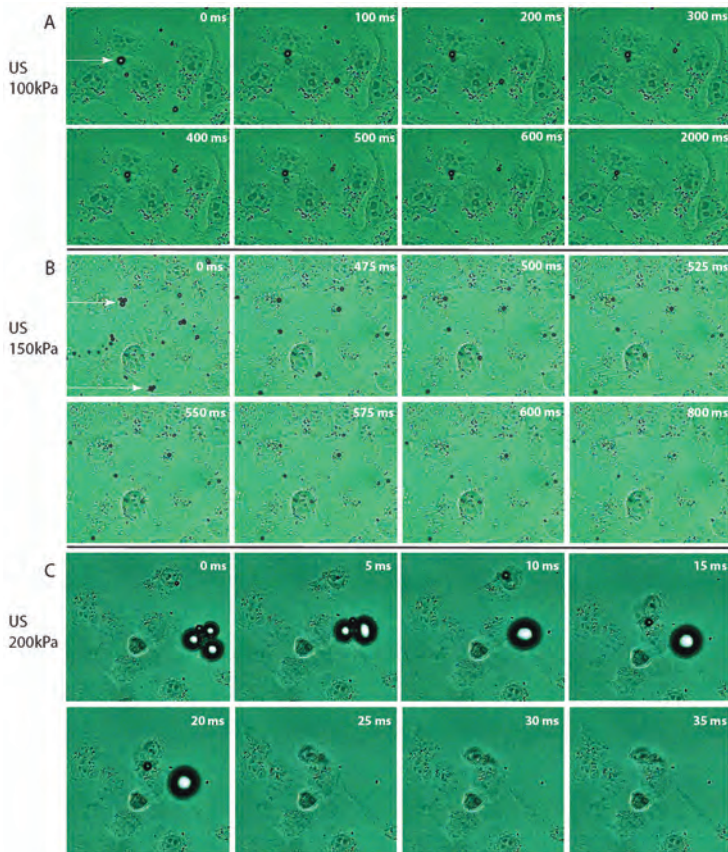


**Figure 4** - Sequences of images of HeLa cells in the presence of microbubbles; (A) images taken during an ultrasound stimulation at 100 kPa, the microbubble surrounded interacts with the plasma membrane by cellular "massage"; (B) images taken during an ultrasound stimulation at 150 kPa, the microbubble surrounded enters the cell after 552 ms; (C) images taken during an ultrasound stimulation at 200 kPa, a microbubble interact with a cell and detaches it from its support. The arrows show the microbubbles to observe over time. The time displayed corresponds to the value after the start of the ultrasound stimulation.

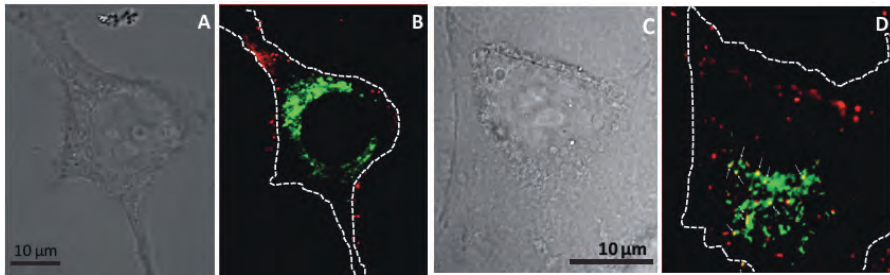


**Figure 5** - Localisation of pDNA relative to late endosomes. HeLa Rab7-eGFP cells were sonoporated at optimal acoustic parameters in presence of 2.5  $\mu\text{g}$  of Cy3-tagged pDNA and microbubble. Green and red staining correspond to Rab7-eGFP positive late endosomes and pDNA-Cy3, respectively. Yellow colour corresponds to a co-localisation of pDNA and Rab7 (arrows). Confocal microscopy observations were made either immediately after sonoporation (A, B) or 3 hours post-sonoporation (C, D). A and C: phase contrast images; B and D: merge of green (Rab7-eGFP) and red (pDNA-Cy3) fluorescence images. White dotted lines in the right frames indicate the cell plasma membrane boundary.

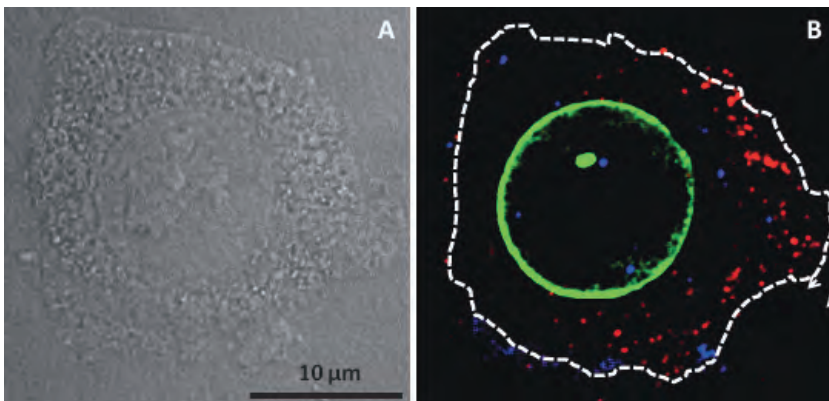


**Figure 6** - Localisation of pDNA relative to the nucleus 6h post-sonoporation. HeLaNup153-eGFP cells were sonoporated at optimal acoustic parameters in presence of 2.5  $\mu\text{g}$  of Cy3-tagged pDNA and DiD labelled microbubbles (blue). The green staining corresponds to Nup153-eGFP which delimits the cell nucleus. Some plasmids were found close to the nucleus 6 hours after sonoporation. Microbubbles were found in the cytoplasm and even in the nucleus 6 hours after sonoporation. A: phase contrast image, B: merge of green (Nup153-eGFP), red (pDNA-Cy3) and blue (MB-DiD) fluorescence images.

### **Plasmid and microbubble intracellular trafficking after sonoporation**

A key to success of this technique lies in understanding mechanism governing microbubble and cell interactions. Real time confocal microscopy investigations were performed on adherent cells using plasmid DNA (pDNA) and microbubbles labelled

respectively with Cy3 (red) and DiD (blue) lipophilic tracer, respectively. The first experiments were done on HeLa cells using pDNA-tagged with Cy3 fluorophore. It was mainly localised as red spots at plasma membrane straightaway following sonoporation. At later time, these spots progressively moved inside cells (not shown). The structures could correspond either to vesicles (endosome) or aggregates like structures upon sonoporation. To distinguish between these two possibilities, kinetic experiments were performed in HeLa cells to investigate if pDNA and microbubbles reached some endocytic organelles upon sonoporation. Data presented in figure 5 were obtained with HeLa cells expressing Rab7-eGFP, the late endosomes marker (green). Late endosomes are, intracellular compartments in which end up internalised molecules before being delivered into lysosomes for degradation. Upon sonoporation, pDNA was localised mainly at the plasma membrane and without co-localisation with Rab7-eGFP (Fig. 5A and 5B). Observations made 3 h post-sonoporation indicated that some of pDNA ended up into late endosomes as demonstrated by the yellow colour (merge of green and red spots) indicating their localisation in Rab7 positive organelles (Fig. 5C and 5D). The presence of punctuate red staining corresponding to pDNA could correspond to pDNA that were either free (present inside the cytosol upon sonoporation) or routed in another intracellular compartments different to late endosomes. Microbubbles labelled with DiD were used to follow their fate in HeLa cells expressing Nup153-eGFP that delimit the cell nucleus. The representative analysis shown in figure 6 was acquired 6 h post-sonoporation. Our observations indicated also that pDNA were not efficiently delivered into the nucleus. However, it is worth noticing that some spots were close to the nucleus as indicated by their localisation in the vicinity of nuclear envelope delimited by Nup153-eGFP. The presence of microbubbles and pDNA inside cells raises the question of their intracellular entry pathway. It must be noted that the amount of pDNA found close to or inside the nucleus was not abundant compared to the pDNA entered into the cell suggesting that many pDNA have been degraded or excreted. The sonoporation efficiency could be improved at this step.

### ***Endocytosis involvement during sonoporation***

To validate the involvement of endocytosis in the process of gene transfer by sonoporation, we tested the effect of depletion of cellular ATP and inhibitors of endocytosis pathways on the sonoporation gene transfer efficiency. The figure 7 presents that the depletion of ATP reduced by 28 times the efficiency of gene transfer by sonoporation, which demonstrates that this process is active. Inhibition by chlorpromazine was dose-dependent decreasing the gene transfer by 3, 5 and 140 times using concentrations of 7.5, 10 and 20  $\mu\text{g/ml}$ . This decrease corresponded to an inhibition of 70, 82 and 99% of the luciferase activity obtained in untreated cells. In contrast using a concentration of 5  $\mu\text{g/ml}$  no significant inhibition was observed. It is to note that a significant toxicity of chlorpromazine at 20  $\mu\text{g/ml}$  was obtained (approximately 30% cell viability). However, a caveolae pathway inhibitor Filipin III had no significant effect on gene transfer by sonoporation. We validated the effectiveness of the endocytosis inhibition protocol by testing the effect on the internalisation of transferrin, a positive control of the clathrin-dependent endocytosis pathway (data not shown). The conditions used allow an inhibition of transferrin in the presence of

chlorpromazine, while little effect was obtained with cells incubated in the presence of Filipin III. The results obtained with chlorpromazine are in the same direction as those obtained by Meijering *et al.*, they observed a 50% inhibition of the transfer of dextran 500 kDa in endothelial cells [7]. In contrast to our results, these authors have observed an inhibition with the Filipin III, this difference could be due to the size of the molecule transferred which was smaller (500 kDa versus 3 MDa) or to the difference in cell type used.

## Conclusion

We have found the optimal ultrasound parameters in our set-up for an efficient gene delivery on HeLa adherent cells. This study showed the cell-microbubbles interactions and the intracellular fate of microbubbles and pDNA during and after the sonoporation process. A set-up combining high speed camera coupled with confocal fluorescence microscopy has allowed us to observe that depending on the acoustic pressure used, some microbubble were forced to enter the cell during sonoporation whilst other were stuck at the plasma membrane. The microbubbles were found to enter in cells only in the best conditions of transfection suggesting that the microbubble entry could be closely correlated to the plasmid DNA entry into the cell. By combining fluorescent pDNA with cellular tools exhibiting fluorescent intracellular compartments, confocal microscopy observations indicated that the pDNA reached the endocytosis pathway as confirmed by their localisation inside late endosomes and the effect of the inhibitors. The next step of our study will be the development of original microbubbles that could both target and deliver efficiently pDNA in a specific site. As long-term perspective, we intend to exploit ultrasound and microbubbles for theranostic purpose by exploiting their combined ability for molecular imaging and drug/gene delivery.

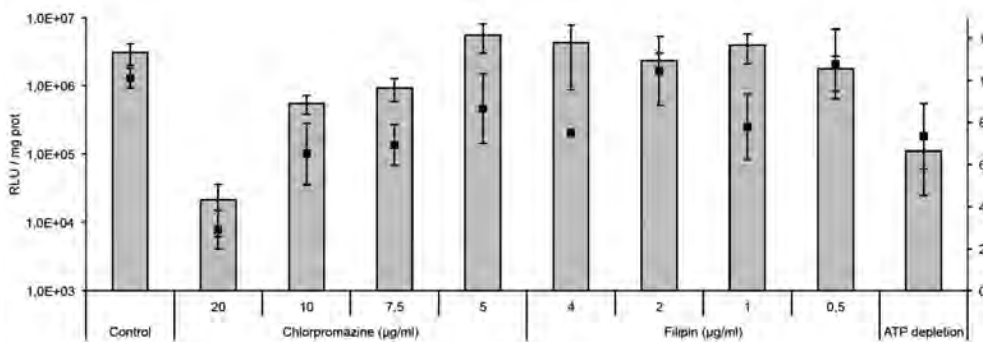


**Figure 7** - Effect of endocytosis inhibitors and cellular ATP depletion on the efficiency of gene transfer by sonoporation. Parameters used: 1 MHz, 60 sec, 150 kPa, 40% DC, 0.3% microbubbles, 10 µg pDNA. The efficacy of gene transfer and the cell viability were determined 24 hours post-sonoporation.

## References

1. Postema, M. and O.H. Gilja, *Ultrasound-directed drug delivery*. Curr Pharm Biotechnol, 2007. **8**(6): p. 355-61.
2. Bao, S., B.D. Thrall, and D.L. Miller, *Transfection of a reporter plasmid into cultured cells by sonoporation in vitro*. Ultrasound Med Biol, 1997. **23**(6): p. 953-9.
3. Miller, D.L., S. Bao, and J.E. Morris, *Sonoporation of cultured cells in the rotating tube exposure system*. Ultrasound Med Biol, 1999. **25**(1): p. 143-9.
4. Taniyama, Y. et al., *Local delivery of plasmid DNA into rat carotid artery using ultrasound*. Circulation, 2002. **105**(10): p. 1233-9.
5. Mehier-Humbert, S. et al., *Plasma membrane poration induced by ultrasound exposure: implication for drug delivery*. J Control Release, 2005. **104**(1): p. 213-22.
6. Kaddur, K. et al., *Transient transmembrane release of green fluorescent proteins with sonoporation*. IEEE Trans Ultrason Ferroelectr Freq Control. **57**(7): p. 1558-67.
7. Meijering, B.D. et al., *Ultrasound and microbubble-targeted delivery of macromolecules is regulated by induction of endocytosis and pore formation*. Circ Res, 2009. **104**(5): p. 679-87.
8. Paula, D.M. et al., *Therapeutic ultrasound promotes plasmid DNA uptake by clathrin-mediated endocytosis*. J Gene Med, 2011. **13**(7-8): p. 392-401.
9. Wang, X. et al., *Gene transfer with microbubble ultrasound and plasmid DNA into skeletal muscle of mice: comparison between commercially available microbubble contrast agents*. Radiology, 2005. **237**(1): p. 224-9.
10. Pichon, C. et al., *Recent advances in gene delivery with ultrasound and microbubbles*. Journal of Experimental Nanoscience, 2008. **3**(1): p. 17-40.
11. Delalande, A. et al., *Ultrasound and microbubbles assisted gene delivery in Achilles tendons: long lasting gene expression and restoration of fibromodulin KO phenotype*. J Control Release, 2011.
12. Suwalski, A. et al., *Accelerated Achilles tendon healing by PDGF gene delivery with mesoporous silica nanoparticles*. Biomaterials, 2009. **31**(19): p. 5237-45.
13. Duvshani-Eshet, M. and M. Machluf, *Efficient transfection of tumors facilitated by long-term therapeutic ultrasound in combination with contrast agent: from in vitro to in vivo setting*. Cancer Gene Ther, 2007. **14**(3): p. 306-15.
14. Li, Y.S. et al., *Optimising ultrasound-mediated gene transfer (sonoporation) in vitro and prolonged expression of a transgene in vivo: potential applications for gene therapy of cancer*. Cancer letters, 2009. **273**(1): p. 62-9.
15. Kaddur, K. et al., *Transient transmembrane release of green fluorescent proteins with sonoporation*. IEEE Trans Ultrason Ferroelectr Freq Control, 2010. **57**(7): p. 1558-67.
16. Rahim, A. et al., *Physical parameters affecting ultrasound/microbubble-mediated gene delivery efficiency in vitro*. Ultrasound Med Biol, 2006. **32**(8): p. 1269-79.